LETTERS

IgH class switching and translocations use a robust non-classical end-joining pathway

Catherine T. Yan[1,2,3,4], Cristian Boboila[1,2,3,4], Ellen Kris Souza[1,2,3,4], Sonia Franco[1,2,3,4], Thomas R. Hickernell[1,2,3,4], Michael Murphy[1,2,3,4], Sunil Gumaste[1,2,3,4], Mark Geyer[2], Ali A. Zarrin[1,2,3,4], John P. Manis[2,5], Klaus Rajewsky[3,5] & Frederick W. Alt[1,2,3,4]

Immunoglobulin variable region exons are assembled in developing B cells by V(D)J recombination. Once mature, these cells undergo class-switch recombination (CSR) when activated by antigen. CSR changes the heavy chain constant region exons (CH) expressed with a given variable region exon from Cμ to a downstream CH (for example, Cγ, Cε or Cα), thereby switching expression from IgM to IgG, IgE or IgA. Both V(D)J recombination and CSR involve the introduction of DNA double-strand breaks and their repair by means of end joining[1,2]. For CSR, double-strand breaks are introduced into switch regions that flank Cμ and a downstream CH, followed by fusion of the broken switch regions[1]. In mammalian cells, the 'classical' non-homologous end joining (C-NHEJ) pathway repairs both general DNA double-strand breaks and programmed double-strand breaks generated by V(D)J recombination[2,3]. C-NHEJ, as observed during V(D)J recombination, joins ends that lack homology to form 'direct' joins, and also joins ends with several base-pair homologies to form microhomology joins[3,4]. CSR joins also display direct and microhomology joins, and CSR has been suggested to use C-NHEJ[5–8]. Xrcc4 and DNA ligase IV (Lig4), which cooperatively catalyse the ligation step of C-NHEJ, are the most specific C-NHEJ factors; they are absolutely required for V(D)J recombination and have no known functions other than C-NHEJ[2]. Here we assess whether C-NHEJ is also critical for CSR by assaying CSR in Xrcc4- or Lig4-deficient mouse B cells. C-NHEJ indeed catalyses CSR joins, because C-NHEJ-deficient B cells had decreased CSR and substantial levels of IgH locus (immunoglobulin heavy chain, encoded by *Igh*) chromosomal breaks. However, an alternative end-joining pathway, which is markedly biased towards microhomology joins, supports CSR at unexpectedly robust levels in C-NHEJ-deficient B cells. In the absence of C-NHEJ, this alternative end-joining pathway also frequently joins *Igh* locus breaks to other chromosomes to generate translocations.

We generated Xrcc4 (X-ray repair complementing defective repair in Chinese hamster cells 4)-deficient B cells by two different and complementary methods to circumvent the fact that Xrcc4 is absolutely required for generation of mature B cells owing to its requirement for V(D)J recombination[9]. One method involved generating Xrcc4-deficient mice ($Xrcc4^{-/-}$)[9,10] that harboured pre-assembled ('knocked in') immunoglobulin heavy chain (IgH, B1-8-HC) and immunoglobulin light chain (IgL, 3–83k-LC) variable-region exons[11] and that were heterozygous or homozygous for a p53 null mutation to rescue neuronal apoptosis and embryonic lethality of the $Xrcc4^{-/-}$ genotype[12]. Because the $p53^{+/-}$ and $p53^{-/-}$ backgrounds gave similar results, we collectively refer to these mice as XP-T/HL (where T indicates targeted germline knockout, H indicates heavy chain knockin, and L indicates light chain knockin). We used the germline gene-inactivation approach to ensure complete absence of Xrcc4 in mature B cells. XP-T/HL mice contained populations of surface IgM^+ splenic B cells (Fig. 1a); however, as expected[5,11], B-cell numbers were relatively low (see Methods) and there were no T cells (data not shown). Therefore, we also inactivated *Xrcc4* specifically in mature B cells by generating mice that harboured one copy of a *loxP*-flanked (floxed) *Xrcc4* allele ($Xrcc4^c$)[10] and one copy of an *Xrcc4* null allele ($Xrcc4^-$) plus a transgene that drives Cre recombinase expression in later stages of the B lineage from a *CD21* promoter[13] (termed *CD21-cre-Xrcc4*$^{c/-}$ mice). *CD21-cre-Xrcc4*$^{c/-}$ mice had normal numbers of IgM^+ splenic B and T cells (not shown). We were unable to detect intact *Xrcc4* genes, transcripts or proteins in cultured *CD21-cre-Xrcc4*$^{c/-}$ B cells (Supplementary Figs 1–4).

To test the role of Xrcc4 in proliferation and CSR in activated B cells, XP-T/HL, *CD21-cre-Xrcc4*$^{c/-}$ or control (HL, $Xrcc4^{+/-}$HL or $Xrcc4^{c/c}$) splenic $B220^+CD43^-$ B cells were cultured for up to 5 days with either anti-CD40 plus interleukin (IL)-4 to stimulate CSR to IgG1 and IgE or bacterial lipopolysacharride (LPS) to stimulate CSR to IgG2b and IgG3. Proliferation of XP-T/HL and *CD21-cre-Xrcc4*$^{c/-}$ B cells was not markedly impaired (Fig. 1b), even though both mutants were highly sensitive to ionizing radiation (Fig. 1c), the latter being consistent with their complete deficiency of Xrcc4. Enzyme-linked immunosorbent assays (ELISAs) for secretion of IgH isotypes in appropriately stimulated XP-T/HL and *CD21-cre-Xrcc4*$^{c/-}$ B cells revealed substantial production of the IgH isotypes assayed (IgG1, IgG2b, IgG3 and IgE) (Supplementary Fig. 5 and Supplementary Table 1). In addition, flow cytometry assays for surface IgG1, IgG2b and IgG3 also revealed substantial switching by appropriately stimulated XP-T/HL or *CD21-cre-Xrcc4*$^{c/-}$ B cells (Fig. 2a and Supplementary Table 2). On the basis of ten different experiments, average levels of IgG1 were at about 25% of those of controls, but sometimes were as high as 50% (Supplementary Table 2). A time course of IgG1 switching in *CD21-cre-Xrcc4*$^{c/-}$ B cells revealed comparable relative IgH switching between mutant and control B cells at 2.5 days when switching was well below peak levels in controls, and at late time points (for example, 4.5 days) when IgH switching was maximal (Supplementary Fig. 6). An enzyme-linked immunospot (ELISPOT) assay, which provides an assessment of the frequency of antibody-secreting cells at the single-cell level[14], revealed switching to IgG1 to occur at 20–50% of control levels and switching to IgG3 at nearly 50% of control levels for XP-T/HL and *CD21-cre-Xrcc4*$^{c/-}$ B cells, as opposed to the negligible switching in cells deficient for activation-induced cytidine deaminase (AID) (Fig. 2b and Supplementary Table 3). Therefore, all three assays demonstrated that Xrcc4-deficient B cells have decreased overall

[1]Howard Hughes Medical Institute, [2]The Children's Hospital, [3]Immune Disease Institute, [4]Department of Genetics, [5]Department of Pathology, Harvard Medical School, Boston, Massachusetts 02115, USA.

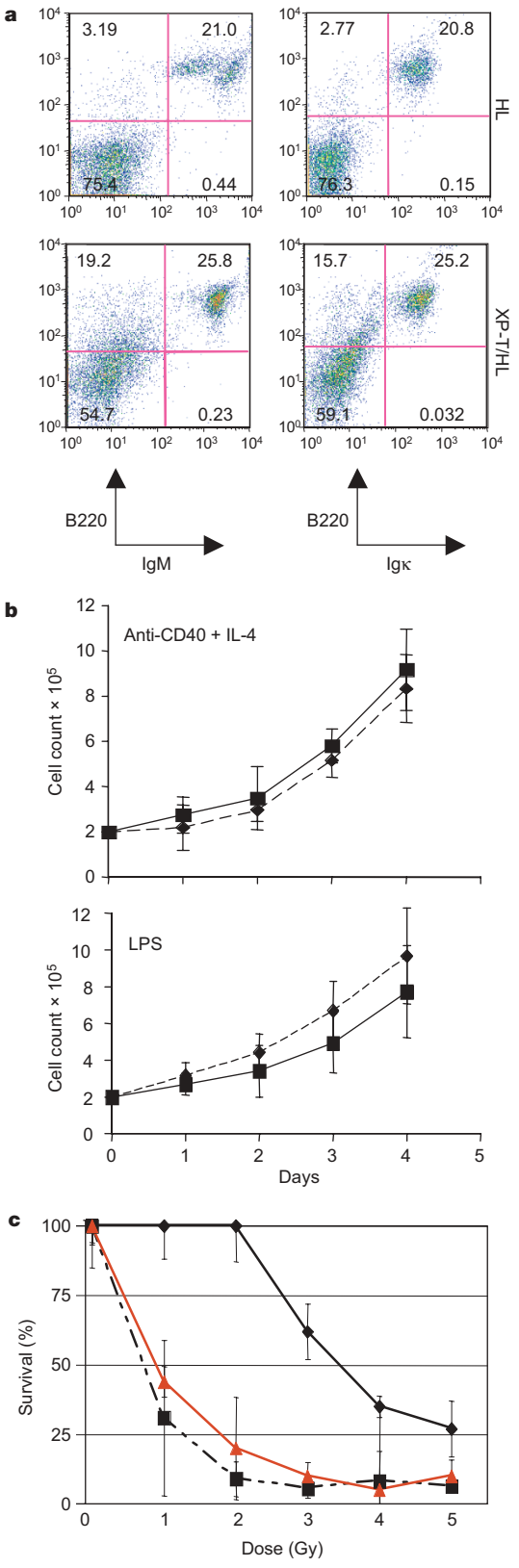

Figure 1 | Proliferation and ionizing radiation sensitivity of Xrcc4-deficient B cells. a, Surface IgM$^+$ and Igκ$^+$ expression on XP-T/HL and HL splenocytes assayed by flow cytometry. **b**, Daily cell counts of activated XP-T/HL (solid line) and HL (dashed line) B cells for three independent experiments. *Xrcc4*$^{c/c}$ and *CD21-cre-Xrcc4*$^{c/-}$ B-cell cultures gave similar results (not shown). Data are presented as mean ± s.e.m. **c**, Ionizing-radiation sensitivity of *Xrcc4*$^{c/c}$ (diamonds), *CD21-cre-Xrcc4*$^{c/-}$ (squares) and XP-T/HL (triangles) B cells activated with anti-CD40 plus IL-4. Representative results of multiple experiments are shown as average per cent survival ± s.e.m. Ionizing-radiation sensitivity of HL cells (not shown) was equivalent to results for *Xrcc4*$^{c/c}$ B cells.

levels of IgH class switching but still carry out this chromosomal end-joining process at robust levels.

NHEJ is catalysed specifically by Lig4, with Xrcc4 serving as a requisite cofactor for activity and stability of the Lig4 protein[15]. Indeed, assays for Lig4 protein in Xrcc4-deficient cells revealed greatly reduced levels (Supplementary Fig. 7), consistent with the identical phenotypes of Xrcc4- and Lig4-deficient cells and mice[9,15,16]. To confirm unequivocally that the high level of CSR observed in Xrcc4-deficient B cells was not caused by some unanticipated Lig4 (and NHEJ) activity, we bred the homozygous Lig4-inactivating mutation[16] into the P-T/HL background to generate LP-T/HL B cells (Supplementary Fig. 8a). The Lig4 mutation deletes much of the *Lig4* gene including the portion encoding the active site of the protein[16]. Notably, LP-T/HL B cells activated with anti-CD40 plus IL-4 still switched to IgG1, as assayed by both surface staining (Fig. 2c and Supplementary Fig. 8b) and ELISPOT (Supplementary Fig. 9), at levels up to 50% of controls. Likewise, the LP-T/HL B cells also underwent switching to IgE (Supplementary Fig. 8c). Therefore, we conclude that there is a robust Xrcc4- and Lig4-independent CSR pathway. In this regard, B cells deficient for Ku70 and Ku80—C-NHEJ factors also required for V(D)J recombination[2]—have severe proliferation defects and a complete inability to undergo CSR[5–7]. Our current findings with Xrcc4- and Lig4-deficient B cells suggest that the more severe phenotypes of the Ku70- and Ku80-deficient cells might reflect functions of Ku proteins in processes other than C-NHEJ[1].

We used fluorescence *in situ* hybridization (FISH) to test whether Xrcc4 deficiency resulted in general and *Igh*-locus-specific chromosomal breaks in XP-T/HL and *CD21-cre-Xrcc4*$^{c/-}$ B cells, as compared to control B cells stimulated with anti-CD40 plus IL-4. On the basis of a telomere FISH (T-FISH) assay[17], both XP-T/HL and *CD21-cre-Xrcc4*$^{c/-}$ B cells exhibited increased levels of general chromosomal aberrations, predominantly chromosome breaks (Fig. 3 and Supplementary Tables 4 and 5); this is consistent with a defect in the repair of double-strand breaks (DSBs) mostly initiated in a pre-replicative cell-cycle phase. To assay for breaks or translocations within the *Igh* locus, we used a FISH assay with one probe that recognizes sequences just upstream of the *Igh* V$_H$ domain on the telomeric region of chromosome 12 (5′ *Igh* probe) plus a probe that recognizes sequences immediately downstream of the C$_H$ locus (3′ *Igh* probe)[17] (Fig. 3a). This assay revealed chromosomal breaks within the *Igh* locus, visualized as separated 3′ and 5′ *Igh* signals, in a large proportion (20–30% on average) of metaphases from activated XP-T/HL and *CD21-cre-Xrcc4*$^{c/-}$ B cells, in contrast to low levels in the control cells (Fig. 3 and Supplementary Tables 4 and 5). Additional FISH analyses mapped many of the *Igh* locus breaks in *CD21-cre-Xrcc4*$^{c/-}$ B cells to a region downstream of Cμ and upstream of Cα, consistent with an origin during attempted CSR (Supplementary Fig. 10). These findings demonstrate that Xrcc4 is required for repair of a subset of *Igh* locus breaks that occur during CSR. Notably, a significant proportion (over 20% on average) of *Igh* locus breaks that did not participate in CSR in XP-T/HL and *CD21-cre-Xrcc4*$^{c/-}$ B cells participated in translocations (Fig. 3d, e and Supplementary Table 5). Thus, in the absence of Xrcc4, another pathway in B cells activated for CSR robustly catalyses translocations of unrepaired *Igh* locus breaks.

End-joining assays on transfected DNA substrates implicated an alternative end-joining pathway that is biased towards microhomology and operates independently of known C-NHEJ factors[4,18–21]. Alternative end-joining also has been implicated in oncogenic translocations in Xrcc4- or Lig4-deficient cells[22]. However, alternative end-joining does not rescue V(D)J recombination in the absence of C-NHEJ factors[9,16] and it has been thought that it does not function efficiently on chromosomal DSBs[4,18,19]. Human B cells that harboured hypomorphic LIG4 mutations showed considerably increased use of microhomology at Sμ to Sα junctions, but not at Sμ to Sγ junctions; this might reflect either increased use of an alternative end-joining pathway or altered activity of residual LIG4

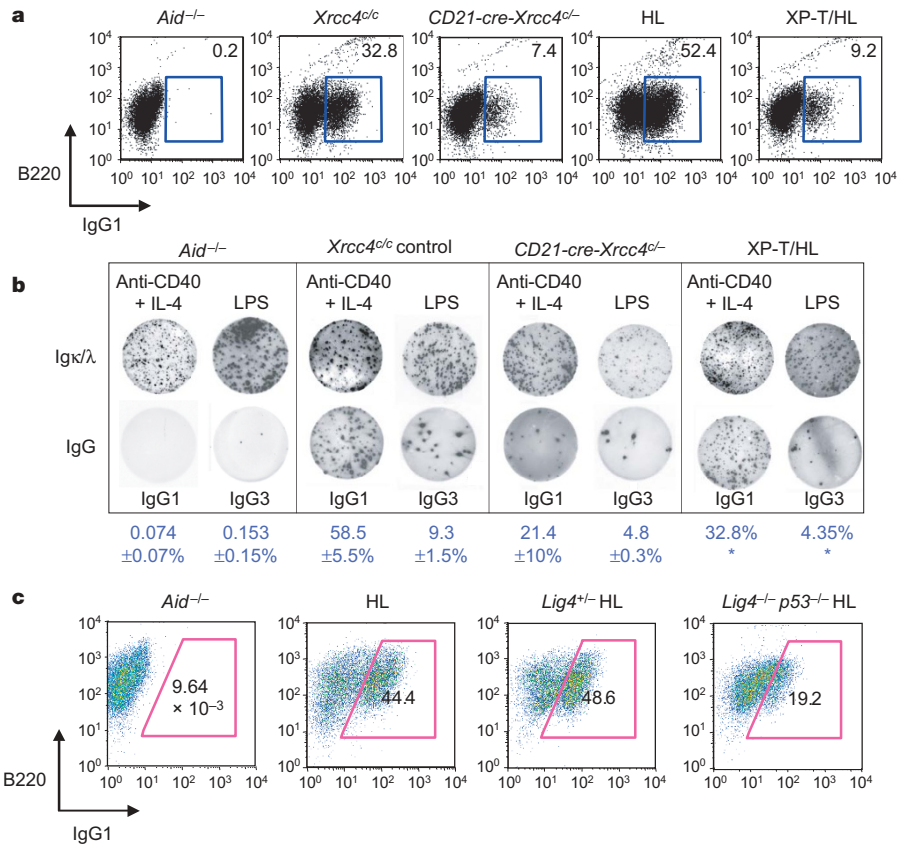

Figure 2 | CSR in Xrcc4-deficient B cells. **a**, Surface IgG1 expression of indicated CD43$^-$ splenic B cells on day four of anti-CD40 plus IL-4 stimulation. (Details of all experiments are in Supplementary Table 2; experiment 7 is shown.) **b**, ELISPOT analysis of switching to IgG1 and IgG3 in Xrcc4-deficient B cells. Average per cent ± s.d. are shown below each panel. Three mice were used for each experiment, except where denoted with an asterisk (in XP-T/HL) where two mice were used. (See Supplementary Table 3 for details.) **c**, Flow cytometric analysis of surface IgG1 expression on day-four anti-CD40- and IL-4-activated Lig4-deficient and control CD43$^-$ splenic B cells (details in Supplementary Fig. 8). AID, activation-induced cytidine deaminase (also known as Aicda).

and C-NHEJ[8]. To determine the nature of the DSB repair pathway that catalyses CSR and translocations in activated XP-T/HL and *CD21-cre-Xrcc4$^{c/-}$* B cells, we analysed CSR junctions. We activated XP-T/HL and control cells with either anti-CD40 plus IL-4 or LPS and then used polymerase chain reaction (PCR) to isolate, respectively, Sμ to Sγ1 and Sμ to Sε junctions or Sμ to Sγ2b and Sμ to Sγ3 junctions (Fig. 4, Supplementary Table 6 and Supplementary Figs 11–14). We also isolated Sμ to Sγ1 junctions from *CD21-cre-Xrcc4$^{c/-}$* B cells and hybridomas stimulated by anti-CD40 plus IL-4 (Supplementary Fig. 15 and Supplementary Table 6). Comparison of CSR junctions from Xrcc4-deficient B cells to those of controls revealed a profound difference. HL control (or *Xrcc4$^{+/-}$*HL) sequences contained about 30–60% direct joins, depending on the downstream switch region, with most of the remainder being short

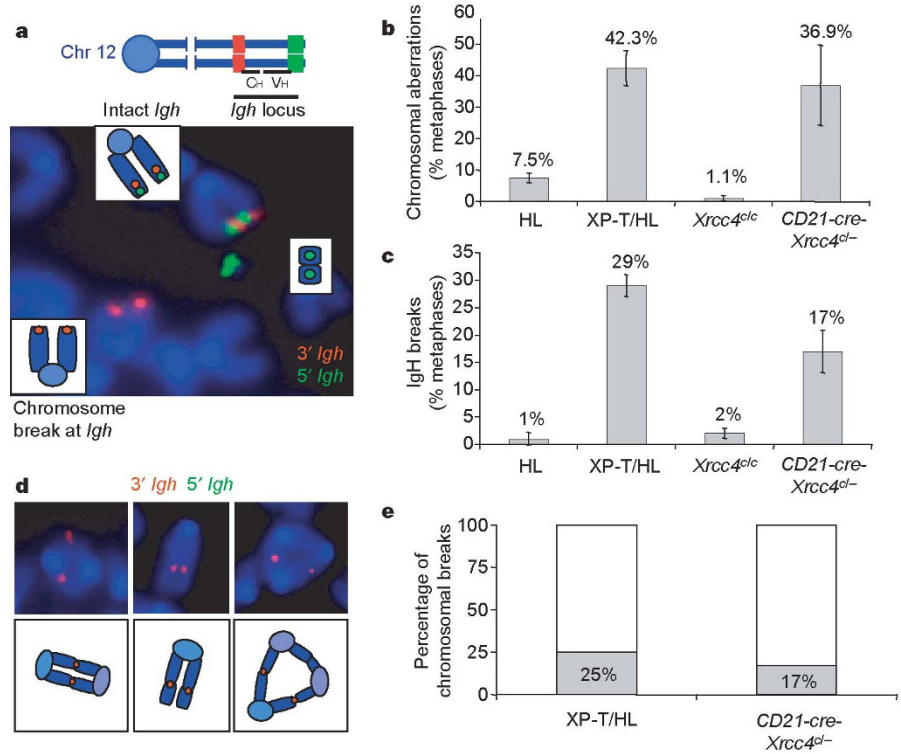

Figure 3 | Frequent general and *Igh*-locus-specific chromosomal breaks and translocations in Xrcc4-deficient B cells. Metaphases from anti-CD40- and IL-4-activated B cells (day four) were analysed by IgH FISH (**a**, **c**–**e**) or T-FISH (**b**) (details in Supplementary Tables 4 and 5). **a**, Representative *Igh* locus breaks in XP-T/HL cultures. Intact *Igh* locus on chromosome 12 shows red and green signals; broken loci show only red or split red and green. **b**, Quantification of general chromosomal breaks. **c**, Quantification of *Igh* locus breaks. Data in **b** and **c** are presented as mean ± s.e.m. **d**, Representative *Igh* locus translocations. **e**, Per cent untranslocated free (clear bars) versus translocated (filled bars) *Igh* locus chromosomal breaks.

(1–4 bp) microhomology joins (Fig. 4 and Supplementary Table 6). In contrast, no direct CSR joins were found in more than 100 junctions from Xrcc4-deficient B cells, regardless of the downstream switch region used (Fig. 4, Supplementary Table 6 and Supplementary Figs 11–15). Most Xrcc4-deficient CSR joins had microhomology ($P = <0.0001$) and the remainder contained insertions of various lengths (Supplementary Table 6) and, as such, also might have been microhomology-mediated. Microhomology joins from Xrcc4-deficient B cells showed an increased distribution of junctions with longer microhomologies than those of the wild type (Fig. 4a–d and Supplementary Table 6), but the distribution of breakpoints within the switch regions and levels of point mutations were similar to those of controls (Supplementary Fig. 16 and Supplementary Table 7). In preliminary studies, a set of analysed Lig4-deficient CSR junctions showed a similar lack of direct joins and a bias towards microhomology joins (C.B., C.T.Y. and F.A., unpublished observations).

We show that an alternative end-joining pathway can join chromosomal DSBs in the physiological context of CSR. Unlike C-NHEJ, this alternative end-joining pathway operates in the absence of Xrcc4 and Lig4 and does not generate readily detectable levels of direct CSR joins. Thus, alternative end-joining is mechanistically distinct from C-NHEJ, both in the use of different ends and of a different ligase, with Lig3 being a likely candidate[18,23]. Until now it has been concluded that alternative end-joining does not function efficiently on chromosomal DSBs, even in the absence of C-NHEJ[4,18,19]. However, we find that this pathway is much more robust in chromosomal DSB repair than previously expected, at least during CSR. Thus, in the absence of C-NHEJ, alternative end-joining catalyses substantial CSR, even early after B-cell activation when CSR is still on the rise. Yet, Xrcc4-deficient B cells are sensitive to ionizing radiation and have increased general genomic instability; this is consistent with our finding that alternative end-joining does not repair all CSR-associated DSBs. It is possible that particular ends favour alternative end-joining, such as those with longer microhomology. Notably, some of the Sμ to Sα junctions in normal human B cells[8] and Sμ to Sε junctions in normal mouse B cells (Supplementary Fig. 14) use long microhomology not characteristic of C-NHEJ[24,25]. Thus, alternative end-joining may compete better with C-NHEJ for CSR events involving switch regions that are relatively homologous in repeat structure (for example, Sμ, Sε and Sα) and which, thereby, provide more optimal microhomology substrates[8]. Furthermore, the increased frequency of CSR junctions with longer microhomologies in certain mismatch-repair-deficient mice[26,27] might reflect alterations in optimal substrate availability that favour alternative end-joining. Our findings raise the question of why alternative

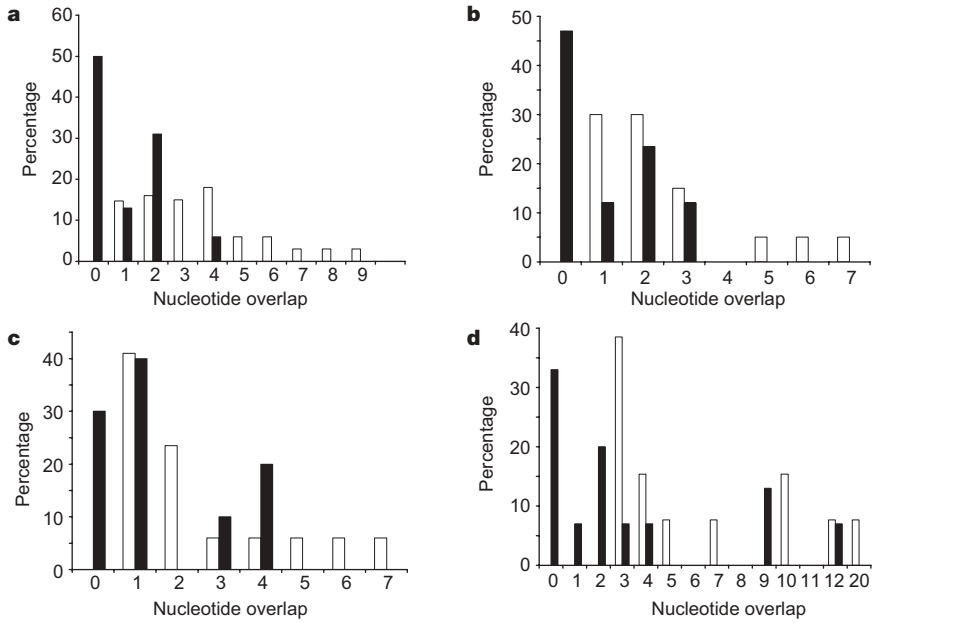

Figure 4 | Structure of Xrcc4-deficient CSR junctions. **a**–**d**, Percentage of sequences with indicated nucleotide (nt) overlap for Sμ and Sγ1 (**a**), Sμ and Sγ2b (**b**), Sμ and Sγ3 (**c**) and Sμ and Sε (**d**) junctions (details in Supplementary Table 6 and Supplementary Figs 11–15). XP-T/HL, open bars; HL, filled bars. **e**, HL (wild type) and XP-T/HL Sμ–Sγ1 junctions (additional sequences in Supplementary Fig. 11). Microhomology is identified as the longest region with perfect homology. GenBank annotated sequence[27] MUSIGD07 (Sμ, top row); CSR junctions (middle row); GenBank sequence MUSIGHANB (Sγ1, bottom row). Vertical line, no sequence identity; blue text with grey highlight, microhomology; underlined blue text, insertions; bold text, point mutations; and dash, deletions. Nucleotide overlaps (black) and insertions (blue) are shown on the right of each sequence.

end-joining does not rescue any V(D)J joining in developing Xrcc4- or Lig4-deficient lymphocytes, despite 50% of normal V(D)J joins having short microhomologies[28]. The answer seems to be provided by recent findings that RAG proteins channel V(D)J DSBs into C-NHEJ and exclude alternative end-joining[31]. In contrast, our current findings show that AID-initiated DSBs during CSR are not similarly restricted to C-NHEJ. Finally, in the absence of C-NHEJ, we find that *Igh* locus CSR breaks are very frequently joined to other chromosomes to generate translocations, which also are probably catalysed largely by alternative end-joining[22]. In this context, alternative end-joining may be inherently 'error-prone'[3,29,30], with this feature being enhanced by frequent occurrence of unrepaired DSBs in the C-NHEJ-deficient background.

METHODS SUMMARY

Generation of XP-T/HL, *CD21-cre-Xrcc4$^{c/-}$* and LP-T/HL mice. XP-T/HL mice (*Xrcc4$^{-/-}$p53$^{+/-}$*HC/LC and *Xrcc4$^{-/-}$p53$^{-/-}$* HC/LC) on the 129 Sv/ev background were generated by breeding *Xrcc4$^{+/-}$ p53$^{+/-}$* with HC/LC (HL) knock-in mice[11]. HL and *Xrcc4$^{+/-}$*HL mice were generated as control cohorts. *CD21-cre-Xrcc4 $^{c/-}$* and *CD21-cre-Xrcc4$^{c/-}$p53$^{+/-}$* mice were generated by crossing *CD21-cre* transgenic mice[13] harbouring heterozygous deletions of *Xrcc4* and *p53*(*CD21-cre-Xrcc4$^{+/-}$p53$^{+/-}$*) with *Xrcc4* floxed (*Xrcc4$^{c/c}$*) mice[10]. LP-T/HL mice (*Lig4$^{-/-}$p53$^{+/-}$*HC/LC) and *Lig4$^{+/-}$*HL mice were generated by crossing *Lig4$^{+/-}$p53$^{+/-}$* with HL mice. Because of the limited lifespan of the *Xrcc4$^{-/-}$p53$^{+/-}$* genetic background, all XP-T/HL and LP-T/HL experiments were performed at 3–5 weeks of age. *CD21-cre-Xrcc4$^{c/-}$* and *Xrcc4$^{c/c}$* mice were analysed at 6–10 weeks of age.

Mature B-cell purification, *in vitro* culture conditions and CSR assays. CD43^{-} B cells were isolated and cultured as previously described[17]. Cells were maintained daily at 5×10^5 cells ml^{-1} and were sampled on various days for RNA, DNA, protein, flow cytometry[17], ELISA[11] and ELISPOT[14] analysis. RNA isolation, Southern blotting and western blotting were performed as previously described[10].

CSR junction analyses. Sμ–Sγ1, Sμ–Sγ2b and Sμ–Sγ3 junctions were amplified by PCR from genomic DNA prepared from splenic B cells activated with anti-CD40 plus IL-4 for 4 days, as described[27]. At least three independent reactions each from three control and three experimental mice were used to obtain products that hybridized with the Sγ1 probe; two mice each were used for other downstream switch regions. PCR products were cloned into the Topo-TA (Invitrogen) or the pGEM-T vector (Promega), sequenced and analysed using Lasergene software and the NCBI database. The GenBank sequence files used were as follows: MUSIGD07 (for Sμ), MUSIGHANB (for Sγ1), MUSIGD18 (for Sγ3), MMU85373 (for Sγ2b) and MUSIGHAHX (for Sε). Sε primers for Sμ–Sε junctions were: Se1, CAAGTTAAGCTCATGCCAGGTCAA; and Se2, CCAGG-CCAGGCCAGTCCTGCTCAGT. PCR was performed using Sμ–Sγ conditions[27].

Two-colour FISH and telomere-FISH. Metaphase spreads from day-four anti-CD40 plus IL-4 B-cell cultures were prepared. Two-colour FISH to detect *Igh*-locus-specific chromosomal aberrations and telomere staining (T-FISH) to detect general aberrations were performed as previously described[17].

Full Methods and any associated references are available in the online version of the paper at www.nature.com/nature.

Received 3 April; accepted 11 June 2007.
Published online 22 August 2007.

1. Chaudhuri, J. *et al.* Evolution of the immunoglobulin heavy chain class switch recombination mechanism. *Adv. Immunol.* **94,** 157–214 (2007).
2. Rooney, S., Chaudhuri, J. & Alt, F. W. The role of the non-homologous end-joining pathway in lymphocyte development. *Immunol. Rev.* **200,** 115–131 (2004).
3. Roth, D. B. Restraining the V(D)J recombinase. *Nature Rev. Immunol.* **3,** 656–666 (2003).
4. Verkaik, N. S. *et al.* Different types of V(D)J recombination and end-joining defects in DNA double-strand break repair mutant mammalian cells. *Eur. J. Immunol.* **32,** 701–709 (2002).
5. Manis, J. P. *et al.* Ku70 is required for late B cell development and immunoglobulin heavy chain class switching. *J. Exp. Med.* **187,** 2081–2089 (1998).
6. Casellas, R. *et al.* Ku80 is required for immunoglobulin isotype switching. *EMBO J.* **17,** 2404–2411 (1998).
7. Reina-San-Martin, B. *et al.* H2AX is required for recombination between immunoglobulin switch regions but not for intra-switch region recombination or somatic hypermutation. *J. Exp. Med.* **197,** 1767–1778 (2003).
8. Pan-Hammarstrom, Q. *et al.* Impact of DNA ligase IV on nonhomologous end joining pathways during class switch recombination in human cells. *J. Exp. Med.* **201,** 189–194 (2005).
9. Gao, Y. *et al.* A critical role for DNA end-joining proteins in both lymphogenesis and neurogenesis. *Cell* **95,** 891–902 (1998).
10. Yan, C. T. *et al.* XRCC4 suppresses medulloblastomas with recurrent translocations in p53-deficient mice. *Proc. Natl Acad. Sci. USA* **103,** 7378–7383 (2006).
11. Manis, J. P., Dudley, D., Kaylor, L. & Alt, F. W. IgH class switch recombination to IgG1 in DNA-PKcs-deficient B cells. *Immunity* **16,** 607–617 (2002).
12. Gao, Y. *et al.* Interplay of p53 and DNA-repair protein XRCC4 in tumorigenesis, genomic stability and development. *Nature* **404,** 897–900 (2000).
13. Kraus, M., Alimzhanov, M. B., Rajewsky, N. & Rajewsky, K. Survival of resting mature B lymphocytes depends on BCR signaling via the Igα/β heterodimer. *Cell* **117,** 787–800 (2004).
14. Zarrin, A. A. *et al.* Antibody class switching mediated by yeast endonuclease-generated DNA breaks. *Science* **315,** 377–381 (2007).
15. Bryans, M., Valenzano, M. C. & Stamato, T. D. Absence of DNA ligase IV protein in XR-1 cells: evidence for stabilization by XRCC4. *Mutat. Res.* **433,** 53–58 (1999).
16. Frank, K. M. *et al.* Late embryonic lethality and impaired V(D)J recombination in mice lacking DNA ligase IV. *Nature* **396,** 173–177 (1998).
17. Franco, S. *et al.* H2AX prevents DNA breaks from progressing to chromosome breaks and translocations. *Mol. Cell* **21,** 201–214 (2006).
18. Wang, H. *et al.* DNA ligase III as a candidate component of backup pathways of nonhomologous end joining. *Cancer Res.* **65,** 4020–4030 (2005).
19. Roth, D. B. Amplifying mechanisms of lymphomagenesis. *Mol. Cell* **10,** 1–2 (2002).
20. Kabotyanski, E. B., Gomelsky, L., Han, J. O., Stamato, T. D. & Roth, D. B. Double-strand break repair in Ku86- and XRCC4-deficient cells. *Nucleic Acids Res.* **26,** 5333–5342 (1998).
21. Guirouilh-Barbat, J. *et al.* Impact of the KU80 pathway on NHEJ-induced genome rearrangements in mammalian cells. *Mol. Cell* **14,** 611–623 (2004).
22. Zhu, C. *et al.* Unrepaired DNA breaks in p53-deficient cells lead to oncogenic gene amplification subsequent to translocations. *Cell* **109,** 811–821 (2002).
23. Audebert, M., Salles, B. & Calsou, P. Involvement of poly(ADP-ribose) polymerase-1 and XRCC1/DNA ligase III in an alternative route for DNA double-strand breaks rejoining. *J. Biol. Chem.* **279,** 55117–55126 (2004).
24. Daley, J. M. & Wilson, T. E. Rejoining of DNA double-strand breaks as a function of overhang length. *Mol. Cell. Biol.* **25,** 896–906 (2005).
25. Gu, J. *et al.* XRCC4:DNA ligase IV can ligate incompatible DNA ends and can ligate across gaps. *EMBO J.* **26,** 1010–1023 (2007).
26. Schrader, C. E., Vardo, J. & Stavnezer, J. Role for mismatch repair proteins Msh2, Mlh1, and Pms2 in immunoglobulin class switching shown by sequence analysis of recombination junctions. *J. Exp. Med.* **195,** 367–373 (2002).
27. Ehrenstein, M. R., Rada, C., Jones, A. M., Milstein, C. & Neuberger, M. S. Switch junction sequences in PMS2-deficient mice reveal a microhomology-mediated mechanism of Ig class switch recombination. *Proc. Natl Acad. Sci. USA* **98,** 14553–14558 (2001).
28. Komori, T., Okada, A., Stewart, V. & Alt, F. W. Lack of N regions in antigen receptor variable region genes of TdT-deficient lymphocytes. *Science* **261,** 1171–1175 (1993).
29. Chen, S. *et al.* Accurate *in vitro* end joining of a DNA double strand break with partially cohesive 3′-overhangs and 3′-phosphoglycolate termini: effect of Ku on repair fidelity. *J. Biol. Chem.* **276,** 24323–24330 (2001).
30. Weinstock, D. M., Richardson, C. A., Elliott, B. & Jasin, M. Modeling oncogenic translocations: distinct roles for double-strand break repair pathways in translocation formation in mammalian cells. *DNA Repair (Amst.)* **5,** 1065–1074 (2006).
31. Corneo, B. *et al.* Rag mutations reveal robust alternative end joining. *Nature* doi:10.1038/nature06168 (this issue).

Supplementary Information is linked to the online version of the paper at www.nature.com/nature.

Acknowledgements We thank D. Schatz for the gift of the Lig4 antibody, M. Alimzhanov, S. Casola and J.-B. Telliez for technical assistance and suggestions, and members of the Alt laboratory for discussions. This work was supported by NIH grants (to F.W.A.), an NIH postdoctoral training grant (to C.T.Y.) and a Long-Term Fellowship of the European Molecular Biology Organization (to S.F.). F.W.A. is an investigator of the Howard Hughes Medical Institute.

Author Contributions F.W.A. and C.T.Y. planned the studies and analysed and interpreted the data. C.T.Y. generated the reagents and performed or oversaw all the experiments described. E.K.S. along with C.T.Y. purified and stimulated XP-T/HL B cells for the studies described. C.B. with C.T.Y. generated and analysed the LP-T/HL mice. E.K.S. generated and analysed (with C.T.Y.) most of the switch junctions and performed all statistical analysis. C.T.Y., T.R.H., S.F. and S.G. analysed metaphases for telomere-FISH and IgH FISH. C.T.Y., T.R.H., E.K.S. and C.B. performed ELISPOT analysis with technical assistance and reagents from A.A.Z. C.B. with E.K.S. isolated and analysed hybridoma sequence junctions; J.P.M. with M.G. provided expertise in B-cell stimulation, fluorescence-activated cell sorting and analysis of sequence junctions; and K.R. provided *CD21-cre* and HL mice and helped interpret data. F.W.A. and C.T.Y. wrote the paper.

Author Information Reprints and permissions information is available at www.nature.com/reprints. The authors declare no competing financial interests. Correspondence and requests for materials should be addressed to F.W.A. (alt@enders.tch.harvard.edu).

METHODS

Generation of XP-T/HL, *CD21-cre-Xrcc4*$^{c/-}$ and LP-T/HL mice. All mice are in the 129 Sv/ev genetic background. The various genotypes were identified by Southern blotting as described[10]. Live B220$^+$/IgM$^+$/Igκ$^+$ peripheral B-cell counts in mice were as follows: $1.2 \pm 0.2 \times 10^6$ in *Xrcc4*$^{-/-}$*p53*$^{+/-}$HL mice ($n = 8$), $31 \pm 4 \times 10^6$ in HL mice ($n = 7$), $29 \pm 4 \times 10^6$ in *Xrcc4*$^{+/-}$HL mice ($n = 2$), and 20×10^6 in *Xrcc4*$^{-/-}$*p53*$^{-/-}$/HL mice ($n = 1$). Live B220$^+$/IgM$^+$/Igκ$^+$ B-cell counts for the two LP-T/HL mice analysed were $\sim 1.0 \pm 0.2 \times 10^6$.

Splenic B-cell cultures. Single-cell suspensions of fractionated CD43$^-$ populations were cultured at 5×10^5 cells ml^{-1} in RPMI medium supplemented with 10% FCS and 500 ng ml^{-1} anti-CD40 antibody (Pharmingen) with 25 ng ml^{-1} mouse recombinant IL-4 (R&D Systems) (or 25 ng ml^{-1} LPS plus 25 ng ml^{-1} IL-4) to assay for switching to IgG1 and IgE, or 25 ng ml^{-1} LPS (Sigma) to assay for switching to IgG3 and IgG2b, as previously described[17]. Cultured cells were maintained daily at a density of 5×10^5 cells ml^{-1}, and sampled on various days for RNA, flow cytometry analyses, ELISA, protein and genomic DNA. Western blotting using a rabbit polyclonal affinity-purified antibody against murine Lig4 antibody[32] was performed at 1:250 in 3% milk/TBS-T.

Cell proliferation and analysis of ionizing radiation sensitivity. Proliferation of Xrcc4-deficient B cells was analysed by daily cell counts of activated XP-T/HL versus HL mice; *Xrcc4*$^{c/c}$ and *CD21-cre-Xrcc4*$^{c/-}$ B220$^+$CD43$^-$ splenic B cells were quantified by trypan blue to exclude dead cells. To determine whether Xrcc4-deficient B cells are sensitive to ionizing radiation, purified CD43$^-$ B cells cultured in anti-CD40 plus IL-4 from a total of $n = 5$ *Xrcc4*$^{c/c}$, $n = 5$ *CD21-cre-Xrcc4*$^{c/-}$, $n = 2$ HL, $n = 1$ *Xrcc4*$^{-/-}$*p53*$^{-/-}$HL and $n = 2$ *Xrcc4*$^{-/-}$*p53*$^{+/-}$HL mice—one or more independent stimulations were performed for each mouse on day 2.5 of activation—were plated as triplicate samples, irradiated with a dose of 0–5 Gy, and counted with trypan blue to exclude dead cells 24 h after irradiation.

Flow cytometry analyses. For fluorescence-activated cell sorting analyses, cells were washed twice in PBS/2% FCS and stained with various antibodies conjugated with fluorescein (IgG1 and IgG2b), phycoerythrin (IgE, IgG3 and IgM) or Cy7-phycoerythrin (B220) as previously described[17]. The cells were analysed by using a FACSCalibur (BD Biosciences), and data were interpreted using FLOWJO software (Tree Star). At least 10,000 events of gated live, lymphoid cells, as determined by forward scatter versus side scatter, were recorded.

ELISA and ELISPOT. ELISAs to detect IgM and various IgG isotypes in cultured supernatants, obtained after 5 days of stimulation, were performed as described[11] using isotype-specific antibodies purchased from Southern Biotechnology Associates. Antibodies for IgE detection were purchased from BD Pharmingen. ELISPOTs were performed essentially as described[14].

Two-colour FISH. Lymphocytes were incubated in colcemid (KaryoMAX, Gibco), swollen in pre-warmed 30 mM sodium citrate for 25 min at 37 °C (or 70 mM KCl for 15 min at 25 °C), fixed in methanol/acetic acid (3/1) and dropped onto slides that were then air-dried overnight. We detected metaphase chromosomes containing the 3′ end of the *Igh* locus using BAC199 (a gift of B. Birshtein) and those containing the 5′ end using BAC207 (a gift of P. Brodeur), and identified chromosomes containing the Cμ–Cδ portion of the locus using an isolated internal 10 kb Cμ/Cδ genomic probe. BACs were labelled with either biotin (biotin-nick translation mix, Roche) or digoxigenin (dig-nick translation mix, Roche), as per the manufacturer's instructions. Two-hundred nanograms of BAC DNA was precipitated with mouse *Cot1* DNA (Invitrogen; ratio of BAC DNA to *Cot1* DNA, 1:20), resuspended in 15 μl of hybridization solution (50% formamide, 2× SSC, 10% dextran sulphate, 0.15% SDS) and co-denatured on slides for 5 min at 76 °C. Slides were then incubated at 37 °C for 16 h, washed in 50% formamide/2× SSC for 5 min twice at 45 °C, then in 2× SSC for 5 min twice at 45 °C and incubated with avidin-Cy3 and antidigoxigenin-FITC (Roche, 1:250 dilution) in 2× SSC/0.05% Tween-20 for 1 h at room temperature (25 °C). After three washes in 2× SSC/0.05% Tween-20, slides were mounted in Vectashield with DAPI (Vector Laboratories). Metaphase images were captured using a Nikon Eclipse microscope equipped with a CCD camera (Applied Spectral Imaging) and a ×63 objective lens. Fifty metaphases were analysed for each sample.

Telomere-FISH. Metaphases on slides were prepared as described above. After pepsin digestion (1 mg ml^{-1} for 10 min at 37 °C), slides were denatured at 80 °C for 3 min, hybridized with a Cy3-labelled PNA telomeric probe (Cy3-$(TTAGGG)_3$) in 70% formamide at room temperature for 2 h, washed, dehydrated and mounted in Vectashield with DAPI (Vector Laboratories). Metaphase images were captured using a Nikon Eclipse microscope equipped with a CCD camera (Applied Spectral Imaging) and a ×63 objective lens. For cytogenetic analysis, 30–40 metaphases per sample were scored for chromosomal aberrations.

32. Jones, K. R. *et al.* Radiosensitization of MDA-MB-231 breast tumor cells by adenovirus-mediated overexpression of a fragment of the XRCC4 protein. *Mol. Cancer Ther.* **4**, 1541–1550 (2005).